Received: 13 July 2020 | Revised: 29 October 2020 | Accepted: 31 October 2020

DOI: 10.1002/ldr.3815

WILEY

RESEARCH ARTICLE

Environmental determinants impacting the spatial heterogeneity of karst ecosystem services in Southwest China

Jiangbo Gao[1] | Liyuan Zuo[1,2] | Wanlu Liu[1,2]

[1]Key Laboratory of Land Surface Pattern and Simulation, Institute of Geographic Sciences and Natural Resources Research, Chinese Academy of Sciences, Beijing, China

[2]College of Resources and Environment, University of Chinese Academy of Sciences, Beijing, China

Correspondence
Jiangbo Gao, No. 11A Datun Road, Chaoyang District, Beijing, China.
Email: gaojiangbo@igsnrr.ac.cn

Funding information
National Natural Science Foundation of China, Grant/Award Numbers: 41671098, 42071288; Programme of Keizhen-Bingwei Excellent Young Scientists of the Institute of Geographic Sciences and Natural Resources Research, Chinese Academy of Sciences, Grant/Award Number: 2020RC002; National Key Research and Development Program of China, Grant/Award Numbers: 2018YFC1508900, 2018YFC1508801

Abstract

Severe rocky desertification and considerable terrain relief in karst areas increase the difficulty of identifying determinants of ecosystem services (ESs), leading to relatively insufficient research on the quantitative attribution of karst ESs. This study investigates environmental determinants and their interactions affecting karst ESs in Southwest China and spatially variable correlations between environmental determinants and karst ESs in geomorphological regions using the geographical detector and geographical weighted regression methodologies. Results show that land use and vegetation coverage are the determinants of water yield and soil loss at the basin scale, with explanatory power of 67.2% and 32.3%, respectively; and the combination of elevation and vegetation coverage determines the spatial distribution of carbon sequestration. The determinants of ESs differed substantially among diverse geomorphological types due to differences in the inner characteristics of each. In addition to the dominant role of land use in each geomorphological type, the effects of vegetation coverage and precipitation on the water yield are significant in mountainous regions. The explanatory power of land use for soil loss decreases with increased terrain relief, while that of the vegetation coverage shows the opposite trend. For carbon sequestration, terrain factors play a more important role than land use at the basin scale, while land use is more influential in each geomorphological type. Furthermore, precipitation and vegetation coverage have the largest impact area on water yield and soil loss in each geomorphological type, respectively, and the impact area of each determinant of carbon sequestration shows obvious regional differences.

KEYWORDS

environmental determinants, karst ecosystem services, quantitative attribution, regional differentiation, spatial heterogeneity

1 | INTRODUCTION

Ecosystem services (ESs) may be defined as 'the natural conditions and utilities provided and maintained by ecosystems that sustain human life' (Daily, 1997). As bridges connecting the natural environment with human well-being, ESs have become a focus of current research in geography and ecology and attracted the attention of many researchers and research organizations (Benson, Jessica, & Darius, 2011; Sutherland et al., 2006; Costanza et al., 2017). In 2001, the United Nations launched the Millennium Ecosystem Assessment (MA), which was a multi-level integrated assessment of the global ecosystem, and the assessment of ESs was its core content (Millennium Ecosystem Assessment, 2005). The MA divided the Earth's land and oceans into 10 systems to analyze ESs, and one of these systems was

Liyuan Zuo is the first co-author contributed equally to this work.

mountains (Zhao & Zhang, 2006). The Intergovernmental Science-Policy Platform on Biodiversity and Ecosystem Services (IPBES), which followed the MA, has attracted increasing attention to ESs around the world (Fu & Zhang, 2014). The IPBES provides a conceptual framework regarding the importance, status, and trends of biodiversity and nature's contributions to people (Intergovernmental Science-Policy Platform on Biodiversity and Ecosystem Services, 2018). As one of the most essential providers of nature's contributions to people, mountains are affected by multiple drivers of change (Martín-López et al., 2019), especially in karst mountain regions, where the ecosystem is fragile and the spatial heterogeneity of ESs is high.

Karst mountain regions, which are characterized by fragile ecosystem, serious rocky desertification and intense human activities, represent one of the most vulnerable ecosystems in the world (Xiong & Chi, 2015). The decline of ESs caused by karst rocky desertification is a major resource and environmental issue that restricts the development of the social economy in karst mountainous areas, which has become a source of great concern to the Chinese Government and scientists (Wang & Li, 2007; Wang, Liu, & Zhang, 2004). Currently, research on karst ESs includes comparative analyses of sample plots using various methods, such as runoff field monitoring, runoff plot experiments, ^{137}Cs analyses and photosynthesis instrumental analyses (Feng et al., 2016). Due to the strong heterogeneity of karst regions, ESs and their determinants present complex features, and it is difficult to extrapolate the results of plot-scale studies to the basin and regional scales (Cai, 2009). At the regional scale, where studying ESs is more meaningful, researchers usually use remote sensing-based empirical formulas or modeling methods, such as the Revised Universal Soil Equation (RUSLE) and Integrated Valuation of Ecosystem Services and Tradeoffs (InVEST) model to study the spatial patterns of ESs and analyze their relationships with environmental factors (Lang, Song, & Deng, 2017; Zeng et al., 2017). However, the current research on the quantitative attribution of ESs is insufficient (Wang & Li, 2007), let alone reveal the spatial heterogeneity and regional differentiation of environmental determinants of ESs in mountainous areas.

The response of ecosystems to direct driving forces varies along spatial and temporal scales and affects the products and services of ecosystems at different scales (Bennet, Peterson, & Gordon, 2009; Duraiappah et al., 2014; Scheffer, Carpenter, Foley, Folke, & Walker, 2001). The diverse geomorphological types, considerable terrain reliefs and strong spatial heterogeneity of mountain terrain have made the non-constant characteristics of karst ESs particularly prominent at different scales (Cai, 2015). In karst mountainous areas, regional conclusions are often difficult to apply to local scales due to significant differences of geological backgrounds and geomorphological characteristics (Cai, 2009), thus indicating regional differentiation. For example, Ma and Zhang (2018) noted that the pattern of soil and water loss varies greatly depending on the slope scale, watershed scale and regional scale. Therefore, a major research challenge is understanding the formation and change mechanisms influencing ESs at different scales. Even within one basin or region, there may be obvious spatial variability in ESs due to changes in the geographical location. For instance, Hou et al. (2018) found that in the upper reaches of the Sancha River basin, where the landform type is plateau, the total runoff and normalized difference vegetation index (NDVI) are mainly positively correlated, while in the downstream peak cluster depression area, these parameters are negatively correlated.

The purpose of this study is to quantitatively identify the environmental determinants of karst ESs in the basin and geomorphological areas and their spatial variability within these regions. This study focuses on three ES variables: water yield, soil loss and carbon sequestration. Due to the advantages of quantitative attribution and the ability to detect compound effects between factors, geographical detector was used to identify the environmental determinants and their interactions of ESs in the basin and different geomorphological areas. The geographical weighted regression (GWR) was applied in each geomorphological type to simulate the spatial correlation between ESs and environmental factors because a local regression method can better identify the correlations between ESs and environmental changes. Quantitatively identifying the correlation between environmental determinants and ESs will provide a scientific basis for the control of rocky desertification and the development of an ecologically sustainable civilization.

2 | MATERIALS AND METHODS

2.1 | Study area

The Sancha River basin (26°06′–27°00′N, 104°54′–106°24′E) is located in southwestern Guizhou Province, China (Figure 1). The basin covers a total area of 4,861 km^2 and has an elevation of approximately 930–2,300 m, and it slopes from the northwest to southeast. The Sancha River, which originates from Wumeng Mountain, is a first-order tributary of the Wujiang River. The Sancha River basin is subject to a subtropical monsoon climate, with rainfall occurring mainly between May and October. The basin is characterized by a typical karst peak-cluster depression, where the risk of rocky desertification is serious. According to the classification of "The Geomorphological Atlas of the People's Republic of China (1: 1 million)", the Sancha River basin includes five geomorphological types, namely: middle elevation plain, middle elevation terrace, middle elevation hill, small relief mountain and middle relief mountain (Zhou & Cheng, 2010).

2.2 | Data used in this study

2.2.1 | Remote sensing data

The map of land use in 2015, which has a 30-m resolution, was interpreted from TM images (http://glovis.usgs.gov) and spot investigations. A digital elevation model (DEM) (Figure 1c) with a spatial resolution of 9 m was downloaded using the 91 Satellite Map Assistant software (Google Earth v6.0.3). The LANDSAT-8 OLI (http://ids.ceode.ac.cn), HJ1A/B CCD and GF1 WFV (http://www.cresda.com/CN) remote sensing images were first subjected to various processing treatments, such as radiometric calibration, atmospheric correction and orthorectification. Then, the NDVI was calculated by the ratio of the difference between the reflection value in the near-infrared band

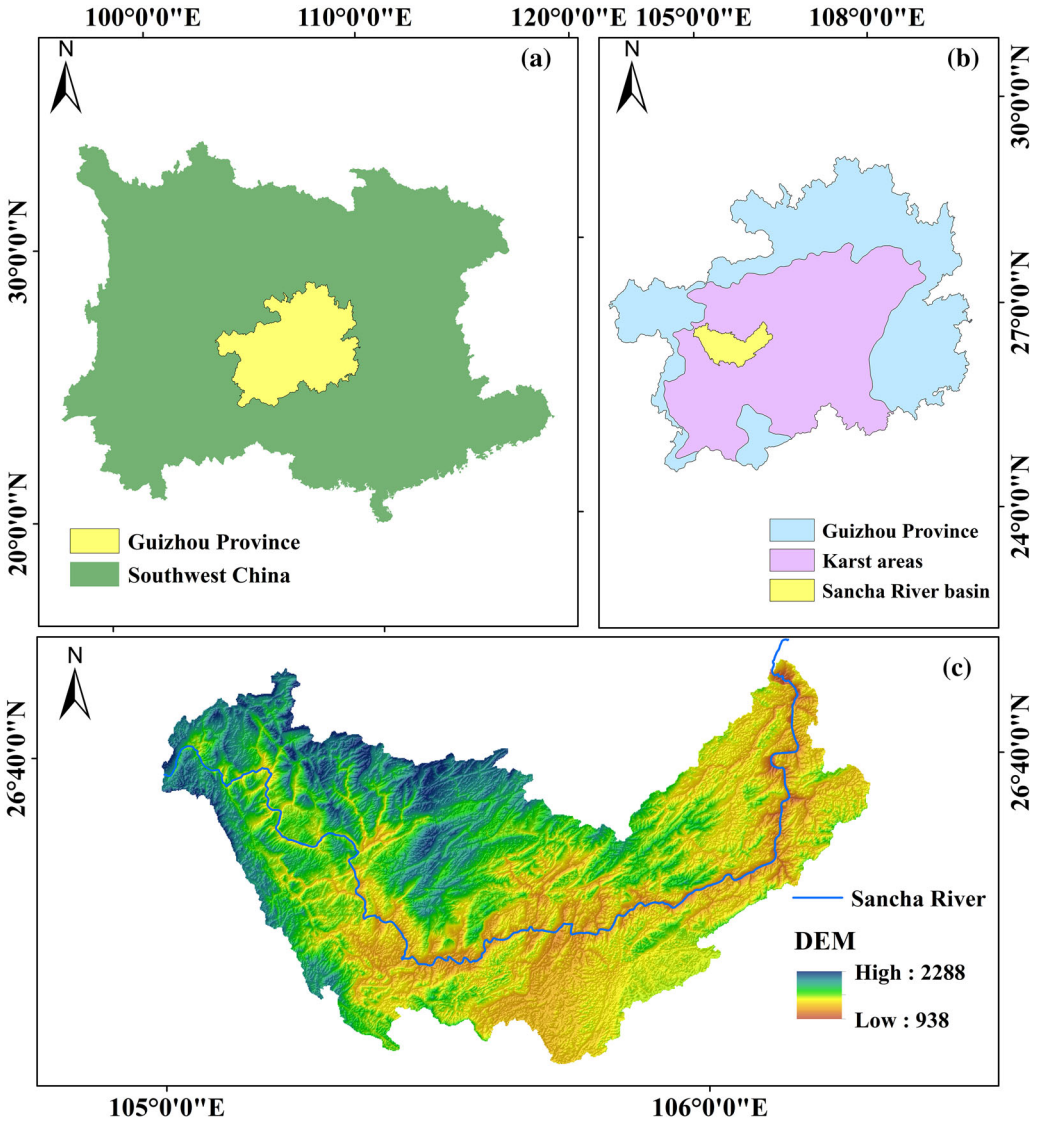

FIGURE 1 The location of the study area (c) in Guizhou Province (b), China (a) [Colour figure can be viewed at wileyonlinelibrary.com]

and the reflection value in the red-band and the sum of the two. Finally, NDVI data with a resolution of 30 m were obtained after various postprocessing treatments, namely, outlier processing, data mosaicking, target area cropping and projection transformation (Figure S1). Comparisons with the MOD13Q1 vegetation index product data showed that the two NDVI data have a good correlation on the temporal scale (R^2 = 0.6). Moreover, from the perspective of spatial distribution, the NDVI values of the two NDVI data show the same spatial distribution trend and the distinction among ground features is more consistent. The geomorphology data is vector data, and the vegetation type data is raster data with a resolution of 1 km. Both of them were obtained from the Resource and Environment Data Cloud Platform, Chinese Academy of Sciences (http://www.resdc.cn).

2.2.2 | Meteorological and hydrological data

Basic meteorological data, such as the daily average temperature and daily total precipitation, were obtained from the China Meteorological Data Services Center (http://data.cma.cn). We selected 29 meteorological stations in the study region and surrounding areas, and they were interpolated into 1 km raster data using ANUSPLIN 4.4 software (Hutchinson & Xu, 2013). Based on the spline interpolation theory of ordinary thin plate and local thin plate, ANUSPLIN can introduce not only independent variables, but also covariates (such as elevation). Hydrological data were obtained from the "Hydrological Yearbook of the People's Republic of China—Hydrological Data of the Yangtze River Basin in Wujiang District", and runoff data from the hydrological stations were used to validate the InVEST model.

2.2.3 | Soil properties data

Soil mechanical composition data were provided by the Cold and Arid Regions Sciences Data Center at Lanzhou, China (http://westdc.westgis.ac.cn). This dataset was obtained from the Harmonized World Soil Database version 1.1 constructed by the Food and Agriculture Organization of the United Nations (FAO) and the International

Institute for Applied Systems Analysis (IIASA), Vienna. The soil depth data were obtained through the Soil Data Center, National Earth System Science Data Sharing Infrastructure, National Science & Technology Infrastructure of China (http://soil.geodata.cn).

To solve the problem of a nonuniform spatial resolution of the model input data, we adopted the scale fusion concept to obtain a uniform resolution dataset (Figure S2). The spatial resolution of the land use data and NDVI data used in this paper is 30 m. Based on this, the spatial resolution of the LS factor calculated based on DEM was upscaled from 9 to 30 m. Meteorological, soil and vegetation data with a resolution of 1 km were downscaled to 30 m.

2.3 | Methods

2.3.1 | Calculation of water yield with the InVEST model

Based on the principle of water balance, the water yield module in the InVEST model was used to estimate the water yield. Considering the climate, terrain, soil properties, land use types and other factors of the study area, the model determines the amount of water yield from each pixel as the precipitation less the fraction of water that undergoes evapotranspiration (Sharp et al., 2020). The formula is as follows:

$$Y(x) = \left(1 - \frac{AET(x)}{P(x)}\right) \cdot P(x), \quad (1)$$

Where: x is a pixel in a raster image and $Y(x)$, $AET(x)$ and $P(x)$ are the water yield, actual evapotranspiration and precipitation on pixel x, respectively. The ratio of $AET(x)$ to $P(x)$ represents part of evapotranspiration, and it is affected by the potential evapotranspiration and a natural climatic-soil parameter.

2.3.2 | Modification and application of the RUSLE

The RUSLE model has been widely applied in various mountainous landscapes (Mallick, Alashker, Mohammad, Ahmed, & Hasan, 2014). However, in karst areas, due to the serious rocky desertification and shallow soil layers, soil loss is usually overestimated in areas with high bedrock bareness (Wang, Cai, Lei, & Zhang, 2010). Based on previous artificial rainfall simulation tests (Dai, Peng, Yang, & Zhao, 2017), this paper introduced the correctional factors of rocky desertification to different degrees (α) to optimize the RUSLE model and make the simulation results more accurate (Gao & Wang, 2019). In addition, Feng et al. (2016) revealed that the root mean square error (RMSE) increases significantly as the accumulated area threshold increases in karst areas, which means that the simulation precision of the RUSLE model requires a high-resolution DEM. Therefore, 9-m high-resolution DEM data were used for calculating the *L* factor in this paper. The formula of the RUSLE model is as follows:

$$A = \left(1 - 0.076^2 \times \alpha\right) R \times K \times \mathrm{LS} \times C \times P, \quad (2)$$

Where: A is the annual soil loss (t hm^{-2} yr^{-1}); α is the correctional coefficient corresponding to each grade of rocky desertification (Table 1); R is the rainfall erosivity factor (MJ mm hm^{-2} hr^{-1} yr^{-1}), calculated according to the method proposed by Renard and Freimund (1994); K is a soil erodibility factor (t hm^2 hr hm^{-2} MJ^{-1} mm^{-1}), calculated by the erosion-productivity impact calculator model proposed by Williams (1990); LS is the combined slope length and slope steepness factor (McCool, Foster, Mutchler, & Meyer, 1987; Zhang et al., 2013); C is the cover and agricultural factor (Cai, Ding, Shi, Huang, & Zhang, 2000); and P is the factor of support practice, for which we adopt previous research results (Zeng et al., 2017). The LS, C and P factors are dimensionless.

2.3.3 | Simulation of carbon sequestration with the CASA model

The Carnegie–Ames–Stanford Approach (CASA) is one of the most widely used models for visually depicting the temporal and spatial variation of net primary productivity (NPP) (Mohamed et al., 2004). The NPP calculation is based on the following expression:

$$\mathrm{NPP}_t = \mathrm{APAR}_t \times \varepsilon_t, \quad (3)$$

Where: t is the period in which NPP is cumulated, such as 1 month; and APAR_t (MJ m^{-2}) is the photosynthetically active radiation absorbed by vegetation, and it is determined by the total solar surface radiation and the fraction of photosynthetically active radiation (FPAR). Studies have shown that FPAR has a good linear relationship with the NDVI and ratio vegetation index (SR) (Potter et al., 1993; Ruimy, Saugier, & Dedieu, 1994). This paper refers to the research method of Los (1998) and takes the average value of $\mathrm{FPAR}_{\mathrm{NDVI}}$ and $\mathrm{FPAR}_{\mathrm{SR}}$ as the estimated value of FPAR. In addition, ε_t (gC MJ^{-1}) is the actual light use efficiency, which is influenced by temperature stress, water stress and the maximum light use efficiency of vegetation (Zhu, Pan, He, Yu, & Hu, 2006). The improvement of the CASA model is that we referred to the improved values of the maximum

TABLE 1 Correctional coefficients of different degrees of rocky desertification

Rocky desertification	None	Potential	Light	Moderate	High	Severe
Bedrock bareness rate (%)	<20	20–30	31–50	51–70	71–90	>90
a	10	25	40	60	80	95

light use efficiency of vegetation proposed by Dong and Ni (2011) in karst areas.

2.3.4 | Geographical detector

The geographical detector is a new statistical tool used to detect and exploit spatial stratified heterogeneity and reveal the underlying determinants (Wang et al., 2010). This method assumes that the study area is characterized by spatially stratified heterogeneity and consistency in the spatial distribution of two variables indicates a statistical correlation between them (Wang & Xu, 2017). The geographical detector includes four detectors: factor detector, interaction detector, risk detector and ecological detector. The factor detector compares the accumulated dispersion variance of each sub-region with the dispersion variance of the entire study region (Wang, Li, et al., 2010). The proportion of the spatial distribution of the dependent variable *Y* that can be explained by factor *X* is measured by the power of the determinant (*q* value); furthermore, as the *q* value increases, the contribution of *X* to *Y* becomes stronger (Luo et al., 2016). The interaction detector can be used to determine whether covariates *X*1 and *X*2 working together will increase or decrease the explanatory power of the dependent variable *Y* or whether the influence of these factors on *Y* is independent (Wang & Xu, 2017). The relationship between the two covariates can be divided into the following categories (Table 2). The *q* statistic is expressed as follows:

$$q = 1 - \frac{\sum_{h=1}^{L} N_h \sigma_h^2}{N\sigma^2}, \quad (4)$$

TABLE 2 Types of interaction between two covariates

Description	Interaction
$q(X1 \cap X2) < \text{Min}[q(X1), q(X2)]$	Weaken, nonlinear
$\text{Min}(q(X1), q(X2)) < q(X1 \cap X2) < \text{Max}[q(X1), q(X2)]$	Weaken, single factor nonlinear
$q(X1 \cap X2) > \text{Max}[q(X1), q(X2)]$	Enhance, double factors
$q(X1 \cap X2) = q(X1) + q(X2)$	Independent
$q(X1 \cap X2) > q(X1) + q(X2)$	Enhance, nonlinear

Where: $h = 1, 2, \ldots, L$ refers to the strata of variables; N and σ^2 represent the total number of samples and the variance, respectively; N_h and ${\sigma_h}^2$ represent the number of samples and the variance in stratum h, respectively; $\sum_{h=1}^{L} N_h \sigma_h^2$ is the sum of the strata variance; and $N\sigma^2$ is the total sum of the variance.

2.3.5 | Geographical weighted regression

The GWR is an extension of the ordinary least squares regression based on the principle of using linear regression analysis to study the spatial relationship between two or more variables with geographical differences (Fotheringham, Brunsdon, & Charlton, 2002). To compare the importance of different factors, the values of ESs and environmental factors were standardized in the range of 0–1, and the land use type was replaced by the standardized land use intensity according to the characteristics of different land use types (Liu, Li, Yi, & Cheng, 2017; Zhuang & Liu, 1997) because type variables cannot be standardized. In this study, the standardized annual water yield, soil loss and carbon sequestration were the dependent variables, and the standardized environmental factors were defined as the independent variables for identifying the spatial heterogeneity in each geomorphological type, where different environmental factors affected karst ESs (Figure 2). The model is expressed as follows:

$$y_i = \beta_0(\mu_i, \nu_i) + \sum_{k=1}^{p} \beta_k(\mu_i, \nu_i) x_{ik} + \varepsilon_i, \quad (5)$$

Where: y_i, x_{ik}, and ε_i represent the dependent variables, independent variables and random errors, respectively; (μ_i, ν_i) refers to the location of point i; k represents the number of independent variables; $\beta_0(\mu_i, \nu_i)$ is the intercept at point i; and $\beta_k(\mu_i, \nu_i)$ is the regression coefficient at point i.

3 | RESULTS

3.1 | Model verification and spatial pattern of ES variables

The water yield simulated by the InVEST model was reliable because the average simulated values of the whole basin were in good

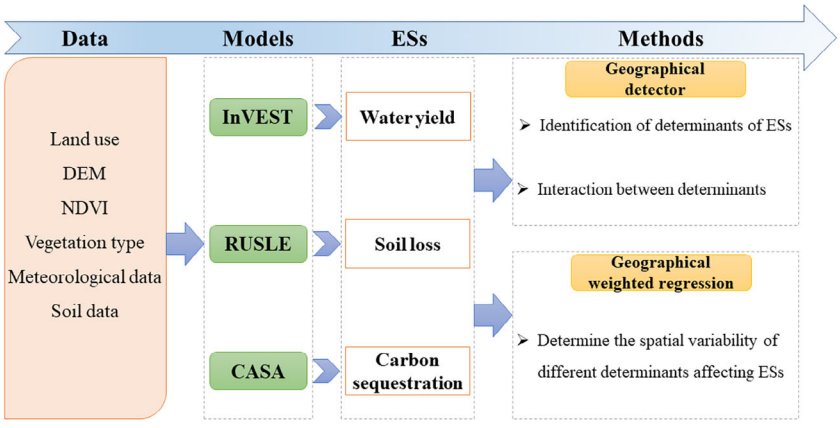

FIGURE 2 Flowchart illustrating the process of calculating ESs and identifying determinants [Colour figure can be viewed at wileyonlinelibrary.com]

agreement with the observed runoff data of hydrological stations in the validation period from 2013 to 2015; that is, the coefficient of determination (R^2) was 0.971 and the Nash-Sutcliffe efficiency (NSE) was 0.845. The spatial distribution of the water yield in the Sancha River basin was characterized by a gradual increase from the southeast to northwest, and the water yield ranged from 206.75 to 1,072.38 mm, with an average of 833.54 mm (Figure 3a). Because of the relatively high precipitation, low temperature and low evapotranspiration in the north-central part of the study area, the water yield was highest in this region.

The average soil loss (3.19 t hm^{-2} yr^{-1}) (Figure 3b) simulated by the RUSLE model was consistent with the result (279.47 t km^{-2} yr^{-1}) for the karst area of Guizhou Province in the 'Water and Soil Conservation Bulletin' in 2015, which was issued by the Water Resources Department of Guizhou Province (http://www.gzmwr.gov.cn/slxw/tzgg/201610/t20161021_1166150.html). According to the classification criterion of soil loss proposed by the Ministry of Water Resources of the People's Republic of China, the soil loss in the Sancha River basin is classified as having a slight grade, and it accounts for 79.95% of the basin area. Regions with soil loss grades above slight are distributed in areas with slopes greater than 35°.

The carbon sequestration calculated by the CASA model in the study area ranged from 0 to 1,035.68 gC m^{-2}, with a mean value of 459.13 gC m^{-2} (Figure 3c). This result is in good agreement with previous studies on carbon sequestration in karst areas (Li, Pan, Wang, Liu, & Zhao, 2014; Zhang, Wang, Liu, Wang, & Yue, 2014). The spatial distribution of simulated carbon sequestration corresponded to the land use type. The land use types in the northwestern part of the study area were mostly forest and grassland, with high vegetation coverage, high maximum light-use efficiency of vegetation and strong photosynthesis; thus, carbon sequestration was high. Due to the lack of vegetation coverage on the surface, the carbon sequestered by waterbodies and construction land was low.

3.2 | Basin-scale analysis of determinants of the karst ESs

The results of the geographical detector showed that the impacts of all environmental determinants on the water yield had strong spatial heterogeneity and the q value of land use was the largest at 0.672, and it was followed by that of elevation, precipitation, vegetation coverage and slope (Table 3). The interaction detector results indicated that land use was still one of the most important factors affecting the water yield, and the top three q values of the interaction were the combination of land use with precipitation, elevation and vegetation coverage, respectively (Table 4), and their explanatory power for the spatial distribution of water yield was more than 70%.

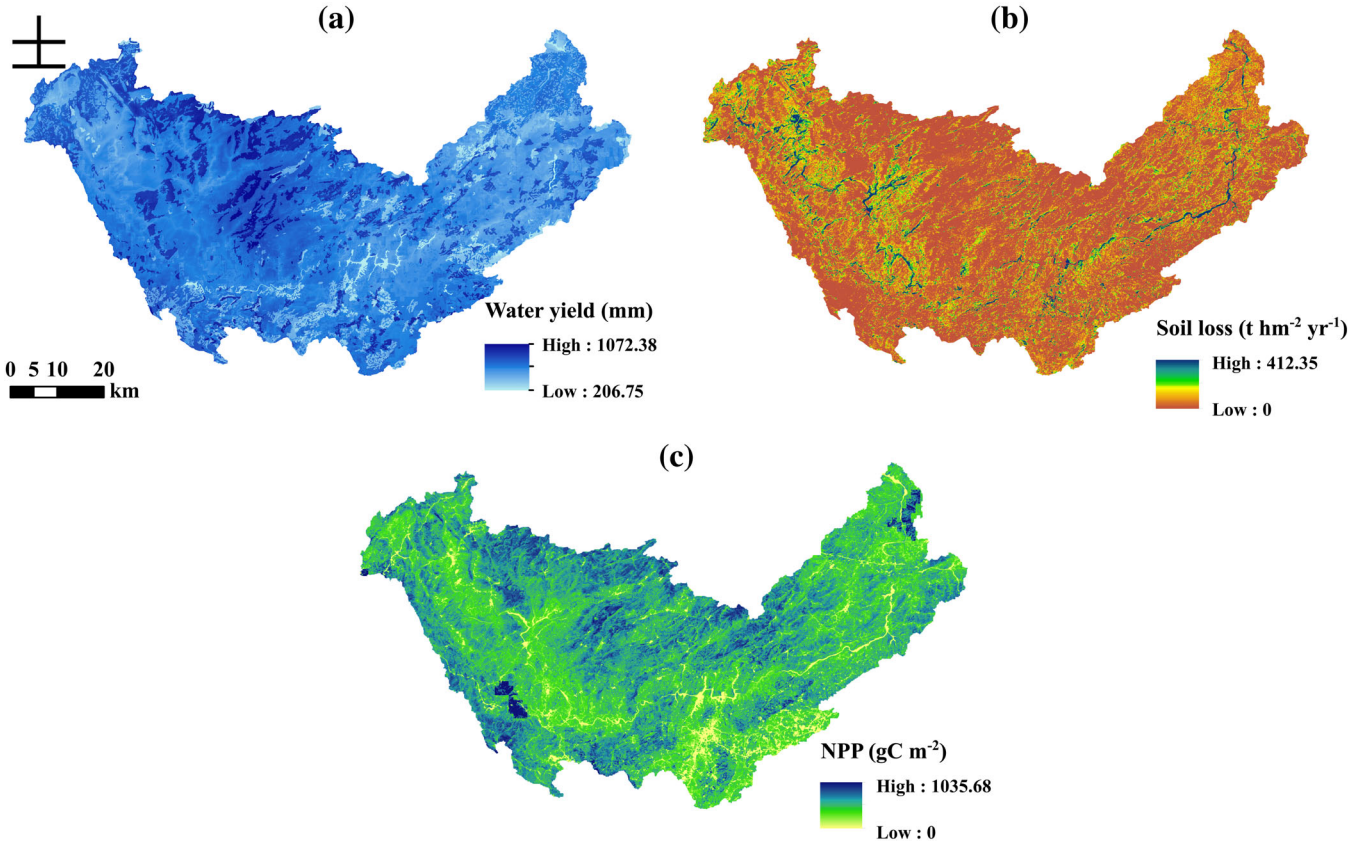

FIGURE 3 The spatial distribution of the water yield (a), soil loss (b), and carbon sequestration (c) [Colour figure can be viewed at wileyonlinelibrary.com]

TABLE 3 The q values of environmental factors affecting spatial distribution of ESs

	Land use	Precipitation	Elevation	Slope	Vegetation coverage
Water yield	0.672	0.157	0.213	0.003	0.068
Soil loss	0.041	0.022	0.028	0.023	0.323
Carbon sequestration	0.171	0.057	0.201	0.107	0.731

TABLE 4 The dominant interactions between two covariates at the basin scale

ESs	Dominant interaction1	Dominant interaction2	Dominant interaction3
Water yield	Landuse ∩ precipitation	Landuse ∩ elevation	Landuse ∩ vegetation coverage
	0.946	0.763	0.702
Soil loss	Vegetation coverage ∩ landuse	Vegetation coverage ∩ slope	Vegetation coverage ∩ precipitation
	0.680	0.559	0.385
Carbon sequestration	Vegetation coverage ∩ elevation	Vegetation coverage ∩ landuse	Vegetation coverage ∩ slope
	0.773	0.746	0.743

The power of vegetation coverage in determining the distribution of soil loss was the largest, q value was 0.323 (Table 3), demonstrating that the vegetation coverage was the most important environmental factor dominating soil loss in the basin. The influences of other environmental factors on soil loss are represented by the order of the q values, which is expressed as land use > elevation > slope > precipitation. The results of the interaction detector showed that interactions between the environmental factors can enhance the explanatory power of the corresponding individual factor to soil loss, and the interactions between vegetation coverage and land use, vegetation coverage and slope, and vegetation coverage and precipitation were the most significant interactions (Table 4). The q values of these combinations were higher than the sum of the single factors.

In addition to vegetation coverage, elevation had the greatest impact on the spatial distribution of carbon sequestration, with a q value of 0.201 (Table 3), which was likely because elevation generally affects regional vegetation patterns by affecting other environmental variables, such as hydrothermal conditions and soil conditions. According to Table 3, the effect of precipitation on carbon sequestration is not significant because the funnel structure formed by karst structures causes most of the precipitation to flow into underground rivers; thus, precipitation is less available to plants (Huang, Lin, Wang, & Chang, 2013). With regard to the interactions between environmental factors, the three dominant interactions were the interactions of the vegetation coverage factor with the elevation, land use and slope, respectively, and their explanatory power for the distribution of carbon sequestration was more than 70% (Table 4).

3.3 | Quantitative attribution of the karst ESs in different geomorphological types

The results of the geographical detector indicated that land use was still the dominant factor affecting the spatial distribution of the water yield among the five geomorphological types (Figure 4a). The minimum q value of land use appeared in the small relief mountain area, with a value of 0.64. In mountainous areas, the q values of vegetation coverage were greater than 10%, which were higher than the q values found in relatively flat areas. This result indicated that high vegetation coverage in mountainous areas had a significant impact on the spatial distribution of the water yield. The q values of precipitation varied among different geomorphological types and showed obvious significance in mountainous and hilly areas. Similar to the results at the basin scale, the interaction between land use and other factors has the most significant effect on the spatial distribution of water yield (Figure 5). Specifically, the interaction between land use and precipitation and the interaction between land use and elevation have the largest explanatory power for water yield in each geomorphological type, accounting for more than 75%.

The explanatory power of land use and vegetation coverage for the spatial distribution of soil loss shows a certain regularity with the increase of terrain relief. The q values of land use decrease with increasing terrain relief, while the q values of vegetation coverage show the opposite trend. Because relatively flat areas are greatly affected by human activities, the explanatory power of land use for the spatial distribution of soil loss has become particularly significant in the middle elevation plain and middle elevation terrace, which have explanatory powers of 26.26 and 24.52%, respectively (Figure 4b). In areas with large terrain relief, vegetation coverage has the greatest explanatory power for soil loss. Regarding the interaction detector results, the interaction between land use and vegetation coverage was the highest among the five geomorphological types and the explanatory power was over 69% (Figure 6). This result indicates that soil loss is closely related to the conservation of soil and water by vegetation and the way humans interfere with soil.

The explanatory power of vegetation coverage for the distribution of carbon sequestration was more than 68% in each geomorphological type (Figure 4c). The effects of elevation on the spatial

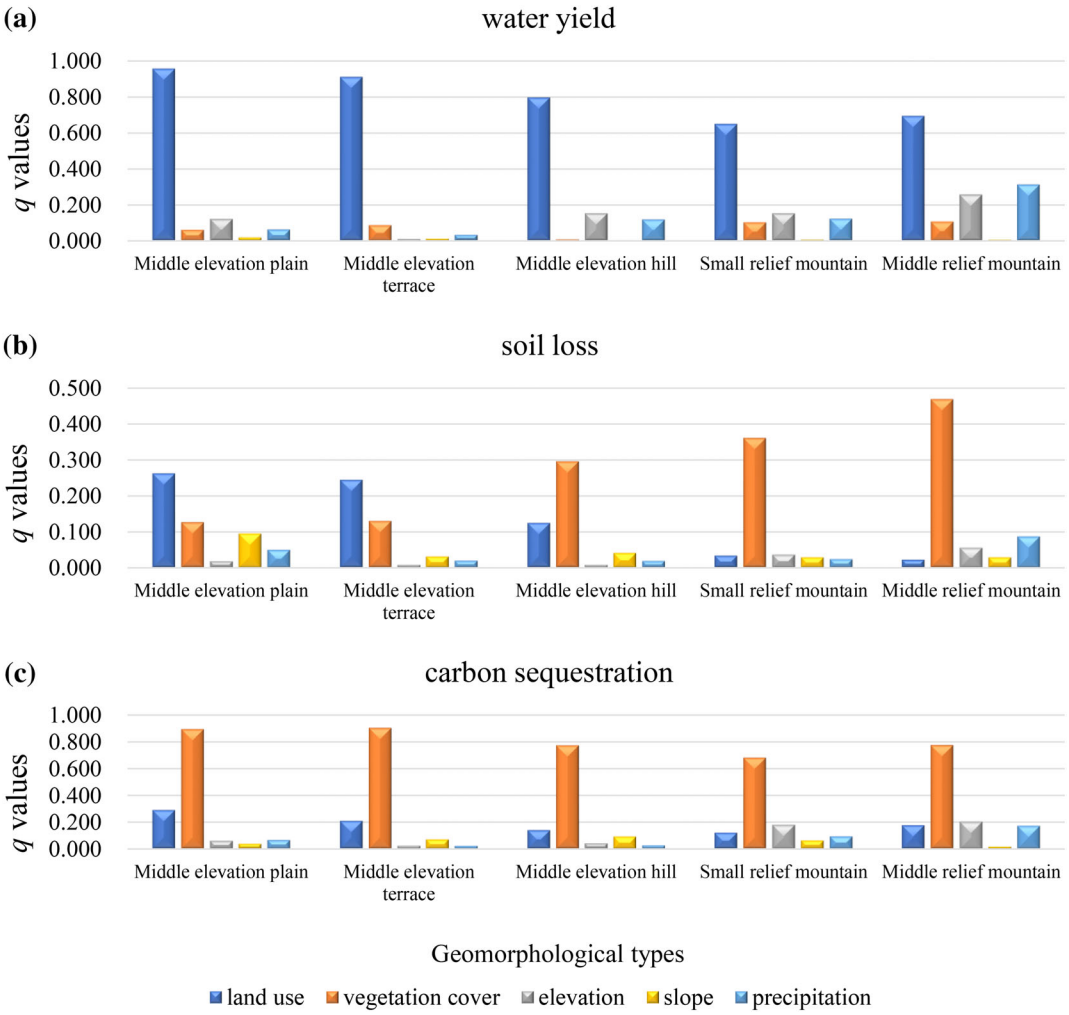

FIGURE 4 *q* values of environmental factors affecting the karst ESs in different geomorphological areas [Colour figure can be viewed at wileyonlinelibrary.com]

Middle elevation plain

	LU	S	VC	E
S	0.961			
VC	0.961	0.137		
E	0.966	0.199	0.245	
P	0.979	0.090	0.155	0.132

Middle elevation terrace

	LU	S	VC	E
S	0.917			
VC	0.916	0.131		
E	0.924	0.019	0.095	
P	0.960	0.044	0.136	0.037

Middle elevation hill

	LU	S	VC	E
S	0.803			
VC	0.800	0.033		
E	0.853	0.170	0.227	
P	0.923	0.142	0.197	0.224

Small relief mountain

	LU	S	VC	E
S	0.653			
VC	0.686	0.124		
E	0.756	0.170	0.233	
P	0.942	0.141	0.249	0.246

Middle relief mountain

	LU	S	VC	E
S	0.704			
VC	0.735	0.127		
E	0.742	0.274	0.297	
P	0.967	0.325	0.340	0.440

High → Low

LU: land use

S: slope

VC: vegetation coverage

E: elevation

P: precipitation

FIGURE 5 The interaction of factors affecting water yield in different geomorphological types [Colour figure can be viewed at wileyonlinelibrary.com]

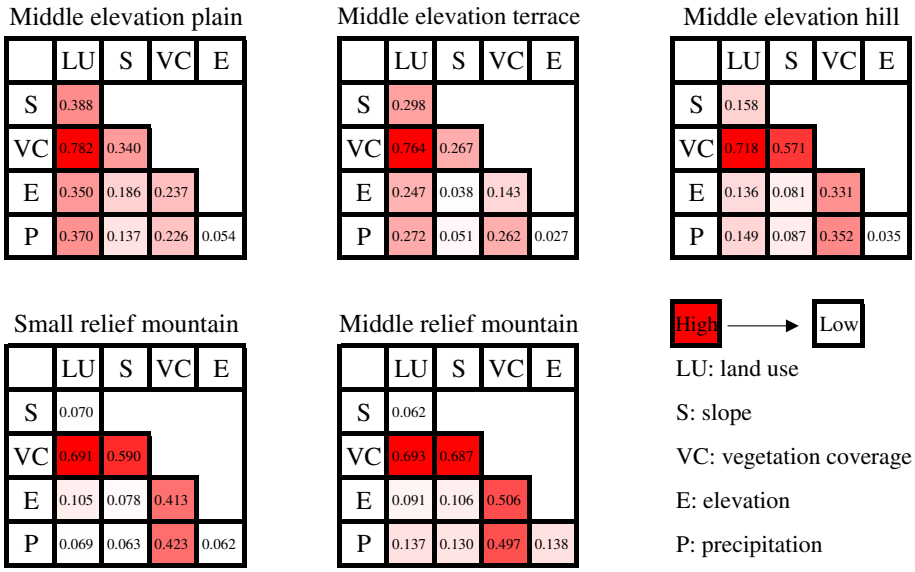

FIGURE 6 The interaction between environmental factors influencing soil loss in different geomorphological types [Colour figure can be viewed at wileyonlinelibrary.com]

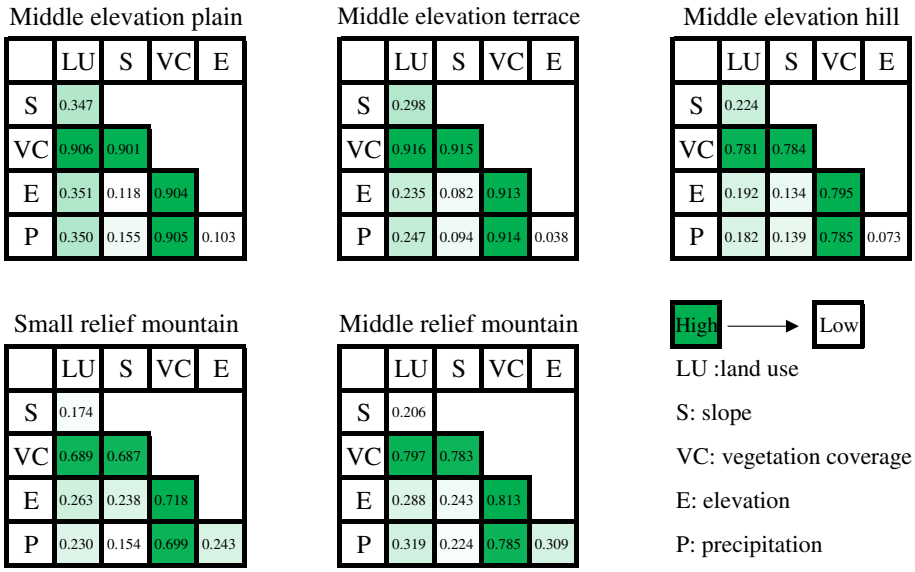

FIGURE 7 The interaction of factors affecting carbon sequestration in different geomorphological regions [Colour figure can be viewed at wileyonlinelibrary.com]

distribution of carbon sequestration showed obvious regional differences, which were manifested in mountainous areas, where the explanatory power of elevation for carbon sequestration was higher than 17%. In contrast, in relatively flat areas, the explanatory power was less than 10%, indicating that elevation played a significant role in the mountainous areas. In the middle relief mountain area, the influence of precipitation on carbon sequestration reached a maximum of 0.172, while in the other four geomorphological types, the influence was not significant. The explanatory power of the slope for the spatial distribution of carbon sequestration was greater than 10% at the basin scale, but for different geomorphological types, the effect of slope was not significant. The results of the interaction detector showed that vegetation coverage also played a dominant role in controlling the spatial distribution of carbon sequestration in different geomorphological types. As shown in Figure 7, the interaction between vegetation coverage and other factors has the highest explanatory power.

3.4 | Spatial variability for impact areas of ESs determinants

After the quantitative attribution of environmental determinants in basin and different geomorphological types, the spatial variability of different environmental determinants affecting the three ESs within each geomorphological region was identified. Impact areas mean that a certain environmental factor most affected karst ESs and its location and spatial distribution in different geomorphological regions were determined by comparing the normalized GWR regression coefficients. The GWR model is applied because independent variables (environmental determinants) and dependent variables (karst ESs) have spatial differences in terms of their geospatial relationships. The results of the spatial autocorrelation analysis show that all Moran's *I* values of the regression parameters of the GWR model selected in this paper are greater than 0 (Table 5), indicating that the selected

TABLE 5 Moran's *I* and *Z* scores of regression parameters for each factor in the GWR model

	Elevation	Vegetation coverage	Land use intensity	Precipitation	Slope
Moran's *I*	0.87	0.29	0.29	0.94	0.16
Z-score	129.97	43.61	42.92	140.98	23.79

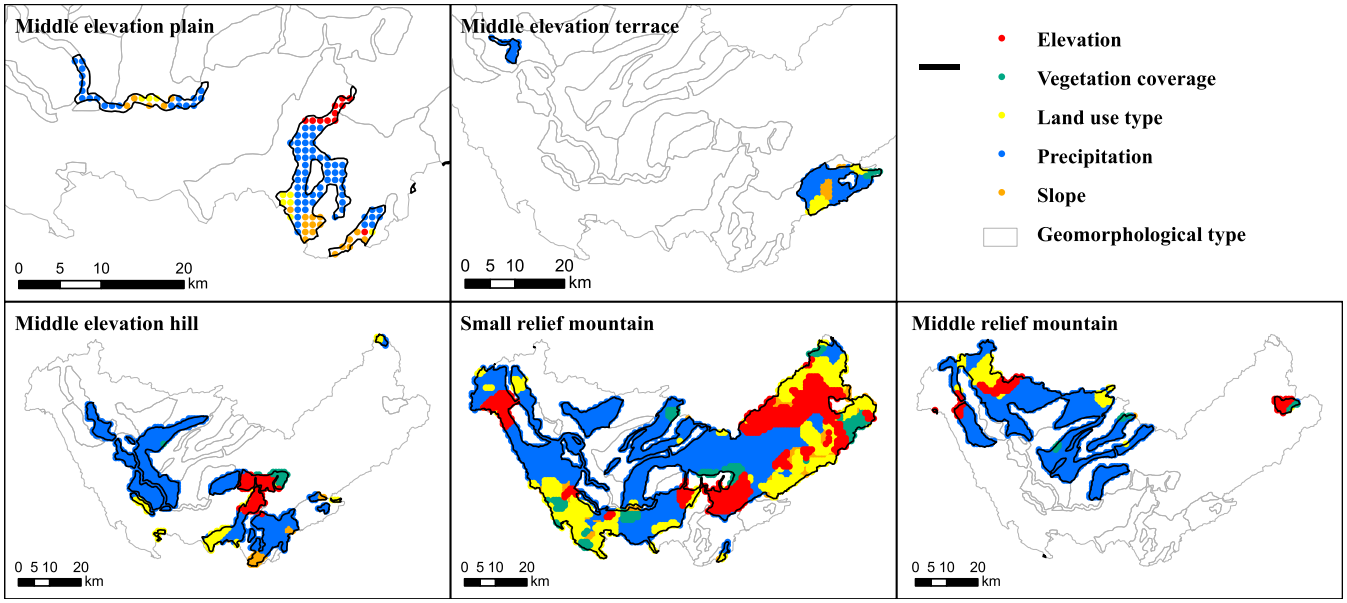

FIGURE 8 Impact areas of environmental factors on water yield in different geomorphological types [Colour figure can be viewed at wileyonlinelibrary.com]

parameters have positive spatial autocorrelations, that is, these parameters are non-stationary in space. The *Z* scores are greater than 2.58, which indicate that they have statistical significance at the 0.01 level. Therefore, the GWR model can be used to identify the spatial distribution of areas where different environmental determinants affected karst ESs.

Figure 8 shows that impact areas of precipitation on water yield accounts for the largest proportion in each geomorphological type. The correlation coefficient between vegetation coverage and water yield in the middle elevation plain is significantly smaller than other factors, indicating that governance measures in this region should focus on the impacts of the other four environmental factors on the water yield. In the other four geomorphological types, the water yield is affected by five environmental factors to varying degrees, and the dominant regions of each environmental determinant factor in the spatial distribution of water yield show obvious spatial heterogeneity. For example, in the small relief mountain area, the impact areas of precipitation are mainly located in the western and central parts, which account for 53.63% of the total area. The area of the land use intensity effect on the water yield is second to that of precipitation in the small relief mountain area, and its impact areas are mainly concentrated in the northern and southwest portions.

Figure 9 revealed that vegetation coverage has the largest impact areas on soil loss compared with other factors in each geomorphological type, which means that improving the vegetation coverage in the study area should be the first priority for soil loss control, thus demonstrating the necessity for ecological engineering implementation. In addition to focusing on the dominant role of vegetation coverage in large portions of the study area, soil loss should also be controlled by zoning according to the factor characteristics of other factor-dominated areas. For example, attention should also be paid to the decisive role of slope in the soil loss in the central part of the middle elevation plain.

The spatial correlation coefficient between vegetation coverage and carbon sequestration is the largest in each geomorphological type. In order to analyze the area of other factors affecting carbon sequestration, we removed the vegetation coverage in Figure 10. In the middle elevation plain, the carbon sequestration on the left is controlled by precipitation and that on the right is controlled by elevation. This result indicated that carbon sequestration should be managed in different zones according to the characteristics of different determinants. Slope has the largest impact area on carbon sequestration in the middle elevation terrace, which means that the influence of slope on vegetation growth and carbon sequestration should be emphasized in this area. In the middle elevation hill area, the dominant area of precipitation was mainly in the central region. The elevation and slope impact areas were mainly concentrated in the eastern part of this geomorphological area. In the small relief mountain area, the precipitation impact areas were mainly concentrated in the western part of the geomorphological area, which accounted for 41.18% of the area. The dominant area of elevation was concentrated in the eastern part of the geomorphological area, which accounted for 45.50% of the area. In the middle relief mountain area, 60.47% of the region was dominated by precipitation.

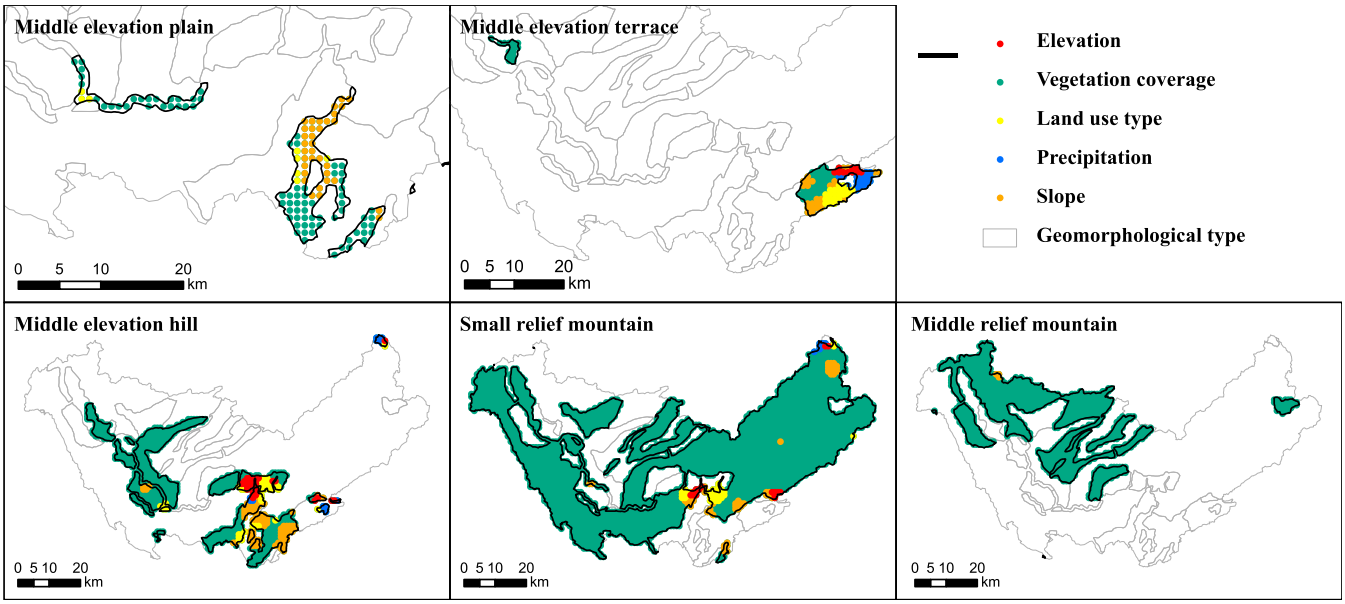

FIGURE 9 Impact areas of environmental factors on soil loss in different geomorphological types [Colour figure can be viewed at wileyonlinelibrary.com]

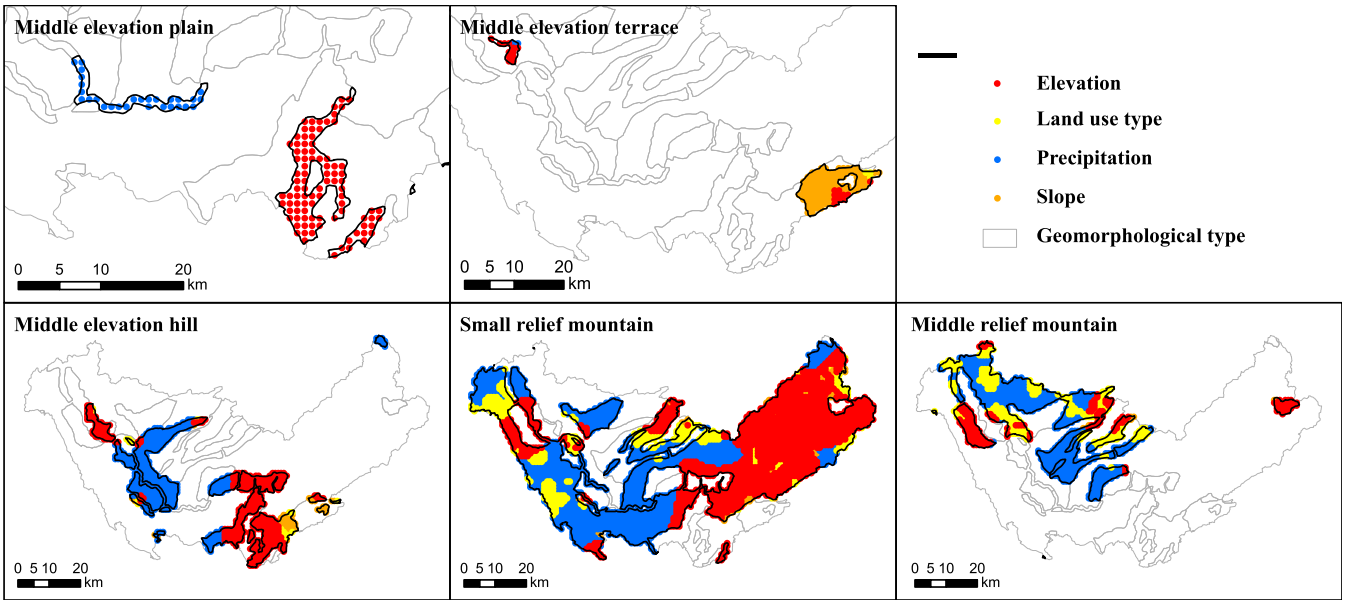

FIGURE 10 Impact areas of environmental factors on carbon sequestration in different geomorphological types [Colour figure can be viewed at wileyonlinelibrary.com]

4 | DISCUSSION

4.1 | Macro-controlling effect of geomorphological features on karst ESs

Geomorphological features play a macro-controlling role in the supply and maintenance of ESs by influencing environmental conditions and ecological processes (Zhao, Liu, Feng, Wang, & Yang, 2018). Soil loss, as a surface process, shows significant differences in terms of erosion characteristics under different geomorphological types. For example, the explanatory power of land use for soil loss decreased as the terrain relief increased, while that of the vegetation coverage showed the opposite trend (Figure 4). Furthermore, the explanatory power of environmental determinants in each geomorphological type differed substantially and that of the elevation for the spatial distribution of carbon sequestration was more pronounced in mountainous areas with high terrain relief. All the results indicate that differences in karst ESs characteristics among diverse geomorphological types should be considered during ES management.

4.2 | Spatial scale characteristics of the impact of determinants on karst ESs

The relationship between ESs and driving forces is often influenced by the temporal and spatial scale (Zhang & Zhao, 2010). Due to the scale characteristics caused by spatial heterogeneity and the complex conversion problems between different scales, the relationships between karst ESs and environmental determinants show obvious regional differentiation at the basin and different geomorphological areas. For example, the impact of land use on the spatial distribution of soil loss is not obvious at the basin scale (Table 3), but in the middle elevation plain and middle elevation terrace, land use becomes the dominant factor and one of the dominant factors in the interactions that affect the spatial distribution of soil loss (Figures 4 and 6). The reason for this pattern is that land use is more fragmented at the basin scale than the geomorphological scale. For certain geomorphological types, humans will intervene in land use according to the geomorphological features, which leads to less differentiation of land use types in the same geomorphological type; thus, land use has more explanatory power regarding the spatial distribution of ESs in different geomorphological regions. This finding proves that the formation of ESs depends on the ecosystem structure and processes on a certain spatial scale and significant leading factors and effects can only be observed at a specific spatial scale (Zhang, Ouyang, & Zheng, 2007), resulting in different orientations and demands of human well-being at different scales. In karst mountain areas, ESs and resource utilization, regional sustainable development and poverty reduction are hot topics in the study of coupling ESs and human well-being. The natural conditions of thin soil, poor soil quality, steep slopes, and more people and less land have caused local people to fall into a vicious cycle of slope reclamation, habitat deterioration, and generational poverty, which is a key area for poverty alleviation. The rational allocation of land use patterns and degrees in different regions, and the research on the driving mechanism of ESs at various scales are the promotion of human well-being and the guarantee of regional ecological security.

Although the spatial heterogeneity of ESs and the regional differentiation of geomorphological types exert influence on the environmental determinants of ESs and their impact areas in space, the intrinsic mechanisms of environmental determinants on ESs still show consistency feature (Figures 8–10). For example, the impact areas of vegetation coverage on soil loss and carbon sequestration accounts for the largest proportion in each geomorphological type. Our result is consistent with the research of Gao, Sun, and Yuan (2010), who found that maintaining and restoring vegetation in karst areas and reducing farming activities were the main ways to control soil loss and rocky desertification. And it also indicates that the implementation of ecological projects, such as the Grain-for-Green Program, have an obvious effect on soil loss.

4.3 | Uncertainty analysis and future perspectives

The spatial autocorrelation and spatial heterogeneity of ecological and geographical phenomena violate the hypothesis of independent and identical distribution in classical statistics (Wang, Li, et al., 2010). However, based on spatial stratification heterogeneity, the geographical detector can detect the quantitative impact of environmental determinants and their interactions on ESs. The GWR model obtains local rather than global parameter estimates (Fotheringham et al., 2002), and it improves the reliability of relationships between ESs and environmental determinants by minimizing the spatial autocorrelation of residuals (Zhang, Gove, & Heath, 2005). Both the geographical detector and GWR methods can effectively reduce information redundancy and collinearity to a certain extent.

The formation and maintenance of ESs depend on the processes of ecological and geographic systems at different spatial and temporal scales (Zhang & Zhao, 2010). An emphasis on the spatial and temporal dimensions represents an important perspective in current ESs research. Studies on multiple time nodes or long time-series should be fully considered in the next step to systematically study the varying relationships between karst ESs and environmental factors under multiple scales to obtain more objective results. Furthermore, the theme of the International Mountain Day, established by the United Nations, has gradually changed from the study of the natural environment to a comprehensive study coupled with human well-being. Therefore, future studies on ESs in karst mountainous areas should take the coupling and the promotion of human well-being into consideration.

5 | CONCLUSIONS

At the basin scale and different geomorphological types, the quantitative attribution of environmental determinants showed that the effect of land use on water yield was stronger than that of other environmental factors, indicating that the water yield supply services in karst areas depend to a large extent on the rational management of land use. Although the impact areas of precipitation on water yield accounts for the largest proportion in each geomorphological type, the effects of elevation and other factors also be given enough attention.

The regional differentiation of geomorphological types makes the determinants of soil loss show obvious differences. Land use is the dominant factor affecting soil loss in the middle elevation plain and middle elevation terrace, while vegetation coverage has the strongest explanatory power for soil loss in mountainous and hilly areas. Furthermore, the explanatory power of land use for soil loss decreased with increasing terrain relief while that of the vegetation coverage showed the opposite trend, indicating that in karst areas with diverse geomorphological types, soil loss and rocky desertification control should be planned based on actual geomorphic characteristics.

Vegetation coverage has the strongest explanatory power and the largest impact area for the spatial distribution of carbon sequestration in the basin and each geomorphological type, which proves the necessity of implementing ecological projects such as the Grain-for-Green Program.

ACKNOWLEDGMENTS

This work was financially supported by the National Natural Science Foundation of China (Grant No. 41671098, 42071288), Programme

of Keizhen-Bingwei Excellent Young Scientists of the Institute of Geographic Sciences and Natural Resources Research, Chinese Academy of Sciences, the National Key Research and Development Program of China (2018YFC1508900, 2018YFC1508801).

CONFLICT OF INTEREST

The authors have no competing interests to declare.

DATA AVAILABILITY STATEMENT

Data available on request from the authors.

ORCID


Jiangbo Gao https://orcid.org/0000-0003-3161-1763

REFERENCES

Bennet, E. M., Peterson, G. D., & Gordon, L. J. (2009). Understanding relationships among multiple ESs. *Ecology Letters*, *12*, 1394–1404. https://doi.org/10.1111/j.1461-0248.2009.01387.x

Benson, C. S., Jessica, M. C., & Darius, J. S. (2011). A GIS application for assessing, mapping, and quantifying the social values of ecosystem services. *Applied Geography*, *31*, 748–760. https://doi.org/10.1016/j.apgeog.2010.08.002

Cai, C. F., Ding, S. W., Shi, Z. H., Huang, L., & Zhang, G. Y. (2000). Study of applying USLE and geographical information system IDRISI to predict soil erosion in small watershed. *Journal of Soil and Water Conservation*, *14*, 19–24 (in Chinese). https://doi.org/10.3321/j.issn:1009-2242.2000.02.005

Cai, Y. L. (2009). Spatial scales integration of land system change: A case study design on Guizhou Karst Plateau. *Advance in Earth Science*, *24*, 1301–1308 (in Chinese). https://doi.org/10.1016/S1874-8651(10)60080-4

Cai, Y. L. (2015). *Study on land change in mountainous areas of Guizhou Karst Plateau*. Beijing: Science Press (in Chinese).

Costanza, R., De Groot, R., Braat, L., Kubiszewski, I., Fioramonti, L., Sutton, P., … Grasso, M. (2017). Twenty years of ESs: How far have we come and how far do we still need to go. *Ecosystem Services*, *28*, 1–16. https://doi.org/10.1016/j.ecoser.2017.09.008

Dai, Q. H., Peng, X. D., Yang, Z., & Zhao, L. S. (2017). Runoff and erosion processes on bare slopes in the karst rocky desertification area. *Catena*, *152*, 218–226. https://doi.org/10.1016/j.catena.2017.01.013

Daily, G. C. (1997). *Nature's services: Societal dependence on natural ecosystems*. Washington, DC: Island Press.

Dong, D., & Ni, J. (2011). Modeling changes of net primary productivity of karst vegetation in southwestern China using the CASA model. *Acta Ecological Sinica*, *31*, 1855–1866 (in Chinese). http://www.ecologica.cn/stxb/ch/reader/view_abstract.aspx?file_no=stxb201002280327.

Duraiappah, A. K., Asah, S. T., Brondizio, E. S., Kosoy, N., O'Farrell, P. J., Prieur-Richard, A. H., … Takeuchi, K. (2014). Managing the mismatches to provide ESs for human well-being: A conceptual framework for understanding the new commons. *Current Opinion in Environmental Sustainability*, *7*, 94–100. https://doi.org/10.1016/j.cosust.2013.11.031

Feng, T., Chen, H. S., Polyakov, V. O., Wang, K. L., Zhang, X. B., & Zhang, W. (2016). Soil erosion rates in two karst peak-cluster depression basins of Northwest Guangxi, China: Comparison of the RUSLE model with 137Cs measurements. *Geomorphology*, *253*, 217–224. https://doi.org/10.1016/j.geomorph.2015.10.013

Fotheringham, A. S., Brunsdon, C., & Charlton, M. (2002). *Geographically weighted regression: The analysis of spatially varying relationships*. Chichester, England: Wiley.

Fu, B. J., & Zhang, L. W. (2014). Land-use change and ESs: Concepts, methods and progress. *Progress in Geography*, *33*, 441–446 (in Chinese). https://doi.org/10.11820/dlkxjz.2014.04.001

Gao, H. D., Sun, Q. Z., & Yuan, Y. (2010). Characteristics of soil erosion for different land types in karst areas. *Bulletin of Soil and Water Conservation*, *30*, 92–96 (in Chinese). https://doi.org/10.13961/j.cnki.stbctb.2010.02.024

Gao, J. B., & Wang, H. (2019). Temporal analysis on quantitative attribution of karst soil erosion: A case study of a peak-cluster depression basin in Southwest China. *Catena*, *172*, 369–377. https://doi.org/10.1016/j.catena.2018.08.035

Hou, W. J., Gao, J. B., Dai, E. F., Peng, T., Wu, S. H., & Wang, H. (2018). The runoff generation simulation and its spatial variation analysis in Sanchahe basin as the south source of Wujiang. *Acta Geographica Sinica*, *73*, 1268–1282. (in Chinese). https://doi.org/10.11821/dlxb201807007

Huang, X. Y., Lin, D. G., Wang, J. A., & Chang, S. (2013). Temporal and spatial NPP variation in the karst region in South China under the background of climate change. *Scientia Silvae Sinicae*, *49*, 10–16 (in Chinese). https://doi.org/10.11707/j.1001-7488.20130502

Hutchinson, M. F., & Xu, T. (2013). Anusplin Version 4.4 User Guide. Retrieved from http://fennerschool.anu.edu.au/files/anusplin44.pdf

Intergovernmental Science-Policy Platform on Biodiversity and Ecosystem Services (2018). Summary for policymakers of the thematic assessment of land degradation and restoration of the intergovernmental science-policy platform on biodiversity and ESs. Retrieved from http://www.indiaenvironmentportal.org.in/taxonomy/term/59723/

Lang, Y., Song, W., & Deng, X. (2017). Projected land use changes impacts on water yields in the karst mountain areas of China. *Physics and Chemistry of the Earth Parts A/B/C*, *104*, 66–75. https://doi.org/10.1016/j.pce.2017.11.001

Li, Y. L., Pan, X. Z., Wang, C. K., Liu, Y., & Zhao, Q. G. (2014). Changes of vegetation net primary productivity and its driving factors from 2000 to 2011 in Guangxi, China. *Acta Ecologica Sinica*, *34*, 5220–5228. https://doi.org/10.5846/stxb201405100952

Liu, Y. X., Li, Y. B., Yi, X. S., & Cheng, X. (2017). Spatial evolution of land use intensity and landscape pattern response of the typical basins in Guizhou Province, China. *Chinese Journal of Applied Ecology*, *28*, 3691–3702 (in Chinese). https://doi.org/10.13287/j.1001-9332.201711.019

Los, S. O. (1998). Linkages between global vegetation and climate: An analysis based on NOAA advanced very high resolution radiometer data. Degree awarded by Vrije Universiteit, Amsterdam, The Netherlands.

Luo, W., Jasiewicz, J., Stepinski, T., Wang, J. F., Xu, C. D., & Cang, X. Z. (2016). Spatial association between dissection density and environmental factors over the entire conterminous United States. *Geophysical Research Letters*, *43*, 692–700. https://doi.org/10.1002/2015gl066941

Ma, Q. H., & Zhang, K. L. (2018). Processes and prospects of the research on soil erosion in karst area of Southwest China. *Advances in Earth Science*, *33*, 30–41 (in Chinese). https://doi.org/10.11867/j.issn.1001-8166.2018.11.1130

Mallick, J., Alashker, Y., Mohammad, A. D., Ahmed, M., & Hasan, M. A. (2014). Risk assessment of soil erosion in semi-arid mountainous watershed in Saudi Arabia by RUSLE model coupled with remote sensing and GIS. *Geocarto International*, *29*, 915–940. https://doi.org/10.1080/10106049.2013.868044

Martín-López, B., Leister, I., Lorenzo Cruz, P., Palomo, I., Grêt-Regamey, A., Harrison, P. A., … Walz, A. (2019). Nature's contributions to people in mountains: A review. *PLoS One*, *14*, 1–24. https://doi.org/10.1371/journal.pone.0217847

McCool, D. K., Foster, G. R., Mutchler, C. K., & Meyer, L. D. (1987). Revised slope steepness factor for the Universal Soil Loss Equation. *Transactions of the ASAE*, *30*, 1387–1396. https://doi.org/10.13031/2013.30576

Millennium Ecosystem Assessment. (2005). *Ecosystems and human well-being*. Washington, DC: Island Press.

Mohamed, M. A. A., Babiker, I. S., Chen, Z. M., Ikeda, K., Ohta, K., & Kato, K. (2004). The role of climate variability in the inter-annual variation of terrestrial net primary production (NPP). *Science of the Total Environment*, *332*, 123–137. https://doi.org/10.1016/j.scitotenv.2004.03.009

Potter, C. S., Randerson, J. T., Field, C. B., Matson, P. A., Vitousek, P. M., Mooney, H. A., & Klooster, S. A. (1993). Terrestrial ecosystem production: A process model based on global satellite and surface data. *Global Biogeochemical Cycles*, *7*, 811–841. https://doi.org/10.1029/93GB02725

Renard, K. G., & Freimund, J. R. (1994). Using monthly precipitation data to estimate the R factor in the revised USLE. *Journal of Hydrology*, *157*, 287–306. https://doi.org/10.1016/0022-1694(94)90110-4

Ruimy, A., Saugier, B., & Dedieu, G. (1994). Methodology for the estimation of terrestrial net primary production from remotely sensed data. *Journal of Geophysical Research Atmospheres*, *99*, 5263–5283. https://doi.org/10.1029/93JD03221

Scheffer, M., Carpenter, S., Foley, J. A., Folke, C., & Walker, B. (2001). Catastrophic shifts in ecosystems. *Nature*, *413*, 591–596. https://doi.org/10.1038/35098000

Sharp, R., Douglass, J., Wolny, S., Arkema, K., Bernhardt, J., Bierbower, W., … Wyatt, K. (2020). InVEST 3.8.8 User's Guide. The Natural Capital Project, Stanford University, University of Minnesota, The Nature Conservancy, and World Wildlife Fund. Retrieved from http://releases.naturalcapitalproject.org/invest-userguide/latest/index.html

Sutherland, W. J., Armstrong-Brown, S., Armsworth, P. R., Tom, B., Brickland, J., Campbell, C. D., … Watkinson, A. R. (2006). The identification of 100 ecological questions of high policy relevance in the UK. *Journal of Applied Ecology*, *43*, 617–627. https://doi.org/10.1111/j.1365-2664.2006.01188.x

Wang, J., Cai, X. F., Lei, L., & Zhang, H. (2010). Laboratory simulation on soil erosion under different bedrock outcrop rate in southwest karst area, China. *Carsologica Sinica*, *29*, 1–5. https://doi.org/10.3724/SP.J.1011.2010.01385

Wang, J. F., Li, X. H., Christakos, G., Liao, Y. L., Zhang, T., Gu, X., & Zheng, X. Y. (2010). Geographical detectors-based health risk assessment and its application in the neural tube defects study of the Heshun region, China. *International Journal of Geographical Information Science*, *24*, 107–127. https://doi.org/10.1080/13658810802443457

Wang, J. F., & Xu, C. D. (2017). Geographical detector: Principle and prospective. *Acta Geographica Sinica*, *72*, 116–134 (in Chinese). https://doi.org/10.11821/dlxb201701010

Wang, S. J., & Li, Y. B. (2007). Problem and development trends about researches on karst rocky desertification. *Advance in Earth Science*, *22*, 573–582 (in Chinese). https://doi.org/10.1007/s11442-007-0020-2

Wang, S. J., Liu, Q. M., & Zhang, D. F. (2004). Karst rocky desertification in southwestern China: Geomorphology, landuse, impact and rehabilitation. *Land Degradation & Development*, *15*, 115–121. https://doi.org/10.1002/ldr.592

Williams, J. R. (1990). The erosion productivity impact calculator (EPIC) model: A case history. *Philosophical Transactions of the Royal Society of London B*, *329*, 421–428. https://doi.org/10.1098/rstb.1990.0184

Xiong, K. N., & Chi, Y. K. (2015). The problems of South China karst ecosystem in southern China and the countermeasures. *Ecological Economy*, *31*, 23–30 (in Chinese). https://doi.org/10.3969/j.issn.1671-4407.2015.01.006

Zeng, C., Wang, S. J., Bai, X. Y., Li, Y. B., Tian, Y. C., Li, Y. W. L. H., & Luo, G. J. (2017). Soil erosion evolution and spatial correlation analysis in a typical karst geomorphology, using RUSLE with GIS. *Solid Earth*, *8*, 721–736. https://doi.org/10.5194/se-2017-1

Zhang, H. F., Ouyang, Z. Y., & Zheng, H. (2007). Spatial scale characteristics of ecosystem services. *Chinese Journal of Ecology*, *26*, 1432–1437 (in Chinese). http://ir.rcees.ac.n./handle/311016/10623

Zhang, H. M., Yang, Q. K., Li, R., Liu, Q. R., Moore, D., He, P., … Geissen, V. (2013). Extension of a GIS procedure for calculating the RUSLE equation LS factor. *Computers and Geosciences*, *52*, 177–188. https://doi.org/10.1016/j.cageo.2012.09.027

Zhang, L. J., Gove, J. H., & Heath, L. S. (2005). Spatial residual analysis of six modeling techniques. *Ecological Modelling*, *186*, 154–177. https://doi.org/10.1016/j.ecolmodel.2005.01.007

Zhang, M. Y., Wang, K. L., Liu, H. Y., Wang, J., & Yue, Y. M. (2014). Impacts of ecological restoration on vegetation carbon storage in the typical karst region of Northwest Guangxi, China. *Chinese Journal Ecology*, *33*, 2288–2295 (in Chinese). https://doi.org/10.13292/j.1000-4890.2014.0138

Zhang, Y. M., & Zhao, S. D. (2010). The millennium ecosystem assessment follow-up a global strategy for turning knowledge into action. *Journal of Natural Resources*, *25*, 522–528 (in Chinese). https://doi.org/10.11849/zrzyxb.2010.03.017

Zhao, S. D., & Zhang, Y. M. (2006). Ecosystems and human well-being: The achievements, contributions and prospects of the Millennium Ecosystem Assessment. *Advance in Earth Science*, *21*, 895–902 (in Chinese). https://doi.org/10.11867/j.issn.1001-8166.2006.09.0895

Zhao, W. W., Liu, Y., Feng, Q., Wang, Y. P., & Yang, S. Q. (2018). ESs for coupled human and environmental systems. *Progress in Geography*, *37*, 139–151 (in Chinese). https://doi.org/10.18306/dlkxjz.2018.01.015

Zhu, W. Q., Pan, Y. Z., He, H., Yu, D. Y., & Hu, H. B. (2006). Simulation of maximum light use efficiency for some typical vegetation types in China. *Science Bulletin*, *51*, 457–463. https://doi.org/10.1007/s11434-006-0457-1

Zhou, C. H., & Cheng, W. M. (2010). Research and compilation of the Geomorphological Atlas of the People's Republic of China (in Chinese). *Geographical Research*, *29*, 970–979. https://doi.org/10.11821/yj2010060002

Zhuang, D. F., & Liu, J. Y. (1997). Study on the model of regional differentiation of land use degree in China. *Journal of Natural Resources*, *12*, 105–111 (in Chinese). https://doi.org/10.11849/zrzyxb.1997.02.002

SUPPORTING INFORMATION

Additional supporting information may be found online in the Supporting Information section at the end of this article.

How to cite this article: Gao J, Zuo L, Liu W. Environmental determinants impacting the spatial heterogeneity of karst ecosystem services in Southwest China. *Land Degrad Dev*. 2020;1–14. https://doi.org/10.1002/ldr.3815